

Accurate Transformer Inrush Current Analysis by Controlling Closing Instant and Residual Flux

Byung Chul Sung, and Seongil Kim

Abstract--This paper proposes a comprehensive process for analyzing accurate transformer inrush current by elaborately controlling the closing instant of a circuit breaker and the level of residual flux in the iron core. The effectiveness of the proposed analyzing process is verified with a laboratory-scaled test system consisting of a 100 kVA 380/320 V Dyn11 three-phase dry-type transformer and a thyristor-based point-on-wave device. Moreover, the measured inrush currents by the proposed process are compared with those calculated by widely accepted inrush current equations. The proposed analyzing process is highly effective to demonstrate the inrush current under the specified energizing condition concerning the closing instant of the voltage and the residual flux in the iron core. The results show that there is a big difference between the measured and calculated inrush currents under the identical energizing condition of the voltage angle with 0° and the residual flux density with approximately 70 %.

Keywords: Controlled switching, demagnetization, inrush current, point on wave, residual flux, transformer.

I. INTRODUCTION

IN an electrical power system, a power transformer plays a vital role in receiving and sending electrical power with the desired voltage level. During transformer energization and de-energization, various transient phenomena can occur that can have significant impacts on the transformer and the power system such as inrush current, ferroresonance, and transient overvoltages [1]–[7].

Among these transients, the inrush current (or a transient excitation current) is one of the representative phenomena during the transformer energization. It is important to accurately calculate the inrush current to ensure reliable protection coordination and transformer design. However, the accurate calculation of its magnitude is a big challenge as it depends on various factors, such as the closing instant of the voltage waveform, residual flux in the iron core, the material and structure of the iron core (B-H curve), among others. Due to this complexity, inrush current equations have been derived by simplifying the non-linear inrush characteristics. The equations allow only for calculating the highest magnitude of the inrush current under the worst condition as the closing instant of the applied voltage with 0° and the maximum

residual flux density with 70 % or 80 % of the rated flux density [1]–[3].

Numerous approaches have been developed to accurately analyze the inrush current. In [8], an automated test platform was created to identify the inrush current. This platform is capable of measuring the inrush current repeatedly by adjusting the closing instant of the voltage using a controllable alternating current (AC) switch (firing thyristor). However, there is no specific method to control the residual flux. References [9]–[12] have researched various strategies of controlled switching to mitigate the magnitude of the inrush current, with their effectiveness proven by simulations and/or measurements. Nevertheless, the proposed studies primarily focus on determining the proper closing time point according to their strategies, rather than the specific closing time point of the circuit breaker (CB). With regards to the residual flux, the method proposed in [13] removes it to minimize the inrush current. For each phase of the transformer, the prefluxing is done by injecting the direct current (DC), causing the flux of each phase to saturate into the positive direction. Shortly after the prefluxing, the CB closes its contact at 180° to make the negative flux, and this procedure is repeated sequentially phase by phase. However, the proposed method has not been verified by measurement, and the CB to control the closing instant precisely has not been implemented in practice.

This paper proposes a process for analyzing the inrush current with greater precision. This involves controlling both the closing instant of the applied voltage to the transformer and the residual flux of the iron core by taking into account its magnetizing characteristics. The study demonstrates that the accuracy of the demonstrated inrush current can be improved with the proposed methods. Furthermore, the conditions of the transformer energization can be controlled to be identical to that of the equations. With the proposed process, the inrush current is also measured in the laboratory-scaled test system with a 100 kVA 380/320 V Dyn11 three-phase dry-type transformer. Moreover, the measurement results obtained from the laboratory-scaled test system with the proposed process are compared to the values calculated by the equations.

II. EQUATIONS OF INRUSH CURRENT

A. Theoretical Background

When a CB is closed for energizing the transformer, the voltage, $v(t)$ in (1), is applied to the transformer terminal and electromotive force (emf) is generated [14], [15].

$$v(t) = V_{peak} \sin(\omega t + \alpha) \quad (1)$$

B. C. Sung is with the Department of Power System Research, Hyundai Electric & Energy Systems, Seongnam, 13553 Republic of Korea (e-mail of corresponding author: sung.byungchul@hyundai-electric.com).

S. Kim is with the Department of Power System Research, Hyundai Electric & Energy Systems, Seongnam, 13553 Republic of Korea (e-mail: seongil.kim@ieee.org).

All authors have contributed equally.

Paper submitted to the International Conference on Power Systems Transients (IPST2023) in Thessaloniki, Greece, June 12-15, 2023.

$$e = -v(t) = -V_{peak} \sin(\omega t + \alpha) \quad (2)$$

$$e = -N \frac{d\phi}{dt} \quad (3)$$

where V_{peak} is the maximum value of the voltage waveform. ω and t are the angular velocity and the time, respectively. α is the energizing angle at the specific point of the voltage, and e is the generated emf. Furthermore, N is the number of turns in the energized winding of the transformer. ϕ is the magnitude of the magnetic flux.

Right after energizing the transformer, the magnetic flux produced from the winding varies suddenly. Also, the integration of the voltage waveform in (1) over time determines the magnitude of the magnetic flux in (5). Equation (5) is derived from (4) which combines (2) with (3)

$$\frac{d\phi}{dt} = \frac{V_{peak}}{N} \sin(\omega t + \alpha) \quad (4)$$

$$\phi = \frac{V_{peak}}{N} \int \sin(\omega t + \alpha) dt = -\phi_{peak} \cos(\omega t + \alpha) + \phi_c \quad (5)$$

$$\phi_c = \phi_r + \phi_{peak} \cos \alpha \quad (6)$$

where ϕ_{peak} is the maximum value of the magnetic flux. ϕ_c is the constant of the integration. The initial condition for the residual flux, ϕ_r , determines the constant, ϕ_c , as (6) at $t = 0$. Finally, the equation to calculate the magnetic flux is derived as (7).

$$\phi = -\phi_{peak} \cos(\omega t + \alpha) + \phi_r + \phi_{peak} \cos \alpha \quad (7)$$

In other words, the energization of the transformer may cause the inordinately sudden increase of the magnetic flux in the iron core. Moreover, this magnetic flux can be saturated depending on the energizing condition of the transformer. From (7), the maximum magnetic flux can be 2 p.u for the rated value, ϕ_{peak} , when the closing instant of the applied voltage waveform, α , is 0° while its minimum value is 1 p.u with the closing instant of 90° without regard for the residual flux, ϕ_r . Eventually, due to the increased and saturated magnetic flux, the high level of the inrush current occurs and its magnitude can be reached up to several to ten times the rated current [2], [3].

B. Analytical Formulas

Analytical formulas that are typically used for calculating the magnitude of the inrush current and the rate of decay are presented in [2]-[5], specifically in (8).

$$i(n) = \frac{\sqrt{2}U}{\sqrt{R^2 + \omega^2 L^2}} \left(\frac{2B_N + B_R - B_S}{B_N} \right) e^{-\frac{R \cdot t_n}{2L}} \quad (8)$$

where U is the root-mean-square voltage across the winding phase. R and L are the winding resistance and the air-core inductance, respectively. Also, in the core, B_N is the rated

magnetic flux density, B_R is the residual flux density, and B_S is the saturation flux density. Lastly, t_n is the time variable.

The formulas, originally derived from single-phase transformer theory, can also be applied to three-phase transformers through the use of an empirical scaling factor. This scaling factor takes into account various factors such as the number of phases, core construction, and coupling of the transformer. For instance, in a delta connected winding, the scaling factor is 1 as each phase generates inrush current independently, much like in a single-phase transformer. As a result, during the worst energizing condition, only one phase experiences high inrush current, resulting in the line current being almost identical to the phase current [3], [16].

Equation (8) incorporates a factor of $2B_N$, which signifies that the magnetic flux can surge up to twice the rated magnetic flux (2 p.u) at the instant of voltage closure with 0° , assuming no residual flux in the core, as indicated in (7). This also implies that the flux level can escalate up to 2.8 p.u if the residual flux is 0.8 p.u. To estimate the first peak value and decay rate of the inrush current, the formulas, especially (8), account for the remaining magnetic flux, $\left(\frac{2B_N + B_R - B_S}{B_N} \right)$, considering only the air-core reactance and applied voltage based on the saturated condition of the iron core [16].

Moreover, in [2] and [3], the calculated results from the analytical formulas are juxtaposed. Notably, the initial peak values of the inrush current derived from the commonly utilized formulas are highly analogous. As a consequence, only the peak value of the inrush current obtained from (8) is compared with the measurement result [2]-[5].

III. TEST SYSTEM SETUP

An initial laboratory-scale test system is shown in Fig. 1. A 100 kVA 380/320 V Dyn11 three-phase dry-type transformer designed as Table I is chosen considering both the voltage and the capacity of the laboratory facilities. The transformer is connected to the grid through HGC500, a magnetic contactor (MC) of Hyundai Electric, as the main breaker and 75 mm² single-core cables. A 4-channel oscilloscope of Teledyne Lecroy is used to measure the voltage of A-phase and all three line currents with CPC-2000-27-BP2, a current probe capable of measuring up to 2000 A. To accurately analyze the inrush current of the transformer, it is measured under energization

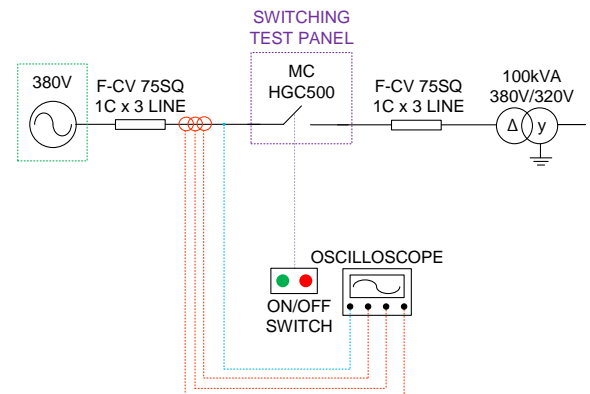


Fig. 1. Configuration of an initial laboratory-scale test system.

conditions that are identical to those specified in (8). For achieving this, as described in the previous section, it is essential to control the closing instant of the applied voltage and the residual flux in the iron core.

The initial test system involves two major drawbacks. Firstly, when energizing the transformer with the operation of the MC in the initial test system in Fig. 1, it may make the closing instant of the voltage uncontrollable. In addition, the mechanical chattering that occurs between the contacts of the MC causes sudden changes in the magnetic flux. Fig. 2 displays the waveforms of the A-phase voltage and line currents that correspond to the operation of the mechanical chattering. The initial portion of the voltage waveform exhibits significant distortion and varies between 360 V and -245 V. As a result, the first peak value of the inrush current from the measured results in the initial test circuit cannot be relied upon.

As a solution, a thyristor switch instead of the MC is applied to the initial test system to control the closing instant of the applied voltage precisely with a function of point-on-wave (POW). Three thyristor switches are made to install individually in every phase, and each single thyristor switch consists of a thyristor and a control board as shown in Fig. 3.

TABLE I
SPECIFICATION OF TRANSFORMER

Capacity [kVA]	100
Phase	3
Frequency [Hz]	60
HV/LV rated voltage [V]	380/320
HV/LV rated phase current [A]	87.72/180.42
%Z	2.61
Connection	Dyn11
Rated magnetic flux density [T]	1.0907

TABLE II
PRINCIPAL ELECTRICAL PROPERTIES OF THYRISTOR

Property	Value
Repetitive peak forward off-state and reverse voltages [V]	1,600
Maximum RMS on-state current [A]	520
Average on-state current [A]	330
Surge current [A]	12,500
Gate controlled delay time [us]	Max. 3

A. Thyristor switch

The thyristor is selected to be suitable for the test system based on its principal electrical properties in Table II. The control board has 6 IN/OUT terminals to link it to the power source for the control board (2 terminals), the emergency ON/OFF (2 terminals), and the external controller (2 terminals), as shown in Fig. 4. Two terminals are respectively made so that every thyristor switch can be connected by one common power source and one emergency ON/OFF controller. One of the rest 2 terminals (Vout) is used to check the operating state of the thyristor by sending a small voltage signal to the external controller after the thyristor is completely closed. The last terminal (Gate ON) receives the operating signal from the external controller, and this signal is transferred to an AND logic gate. The AND logic gate combines the signals from both the external controller and the emergency ON/OFF controller. With ON/OFF signal received from this AND logic gate, a gate driver inside the control board activates the close/open of the thyristor. In other words, only if the external controller and the emergency ON/OFF controller release the ON signal at the same time, the thyristor can be closed. The diagram of the thyristor switch and its application are presented in Figs. 3 and 4, respectively.

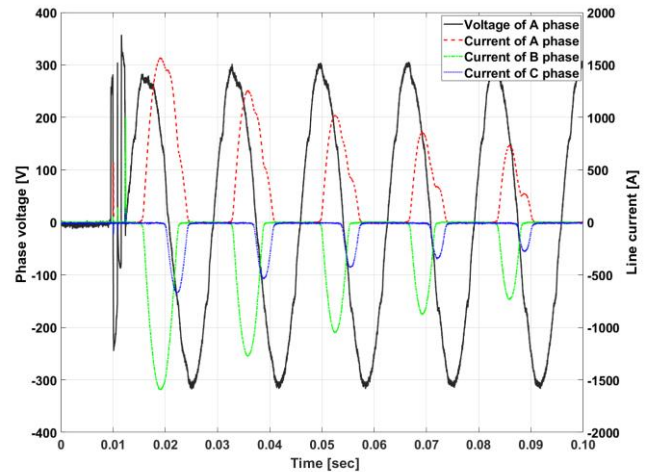


Fig. 2. Measured waveform of A-phase voltage and line currents corresponding to the operation of MC in the initial laboratory-scale test system.

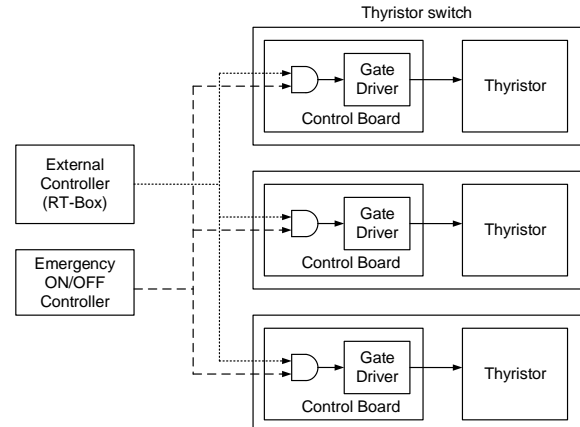
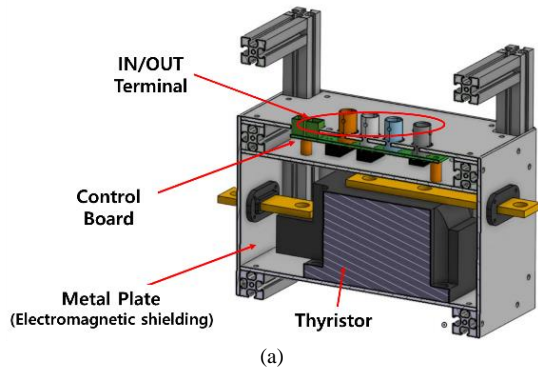
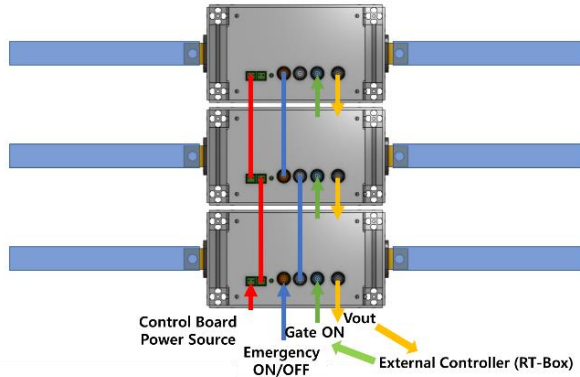


Fig. 3. Simple diagram of thyristor switch.



(a)



(b)

Fig. 4. Thyristor switches: (a) Internal configuration, and (b) Three phase application.

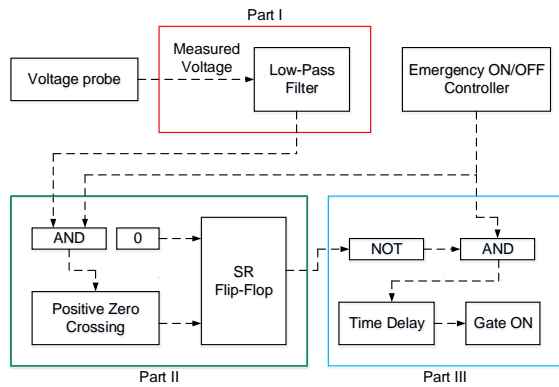


Fig. 5. Logical diagram of the external controller in RT-Box and PLECS.

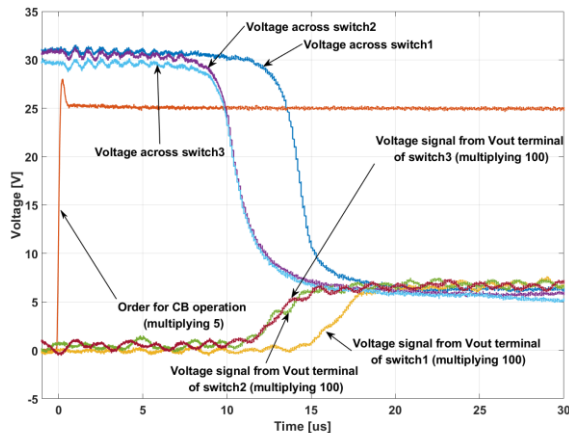


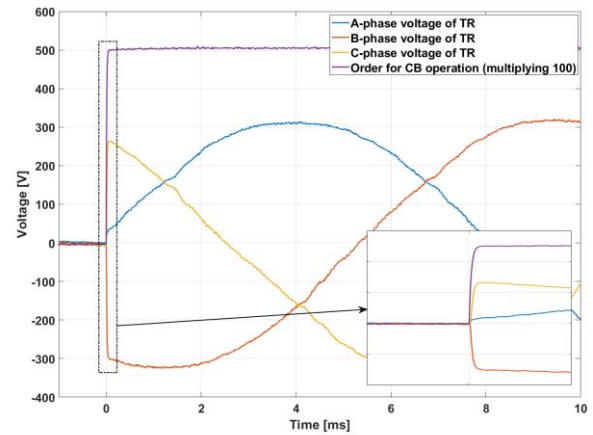
Fig. 6. Verification of operating delay for each thyristor switch.

The external controller is organized for the function of POW by using RT-Box and PLECS, which are a device and a software for real-time simulations. From Fig. 5, there are three major parts in its control logic. In detail, the first part (Part I) takes a voltage measured by the voltage probe and then a low-pass filter suppresses high-frequency components in the voltage to deliver the smoothed voltage to the next part. The second part (Part II) is to check the specific zero-crossing point of the voltage for the required closing instant. In addition, a Set/Reset (SR) flip-flop is applied to close the switches once at the specific instant. The last part (Part III) sends the operating signal after the time, t_o , compensating for the own closing delay of the thyristor switch in (9) according to the required closing instant for 60 Hz voltage.

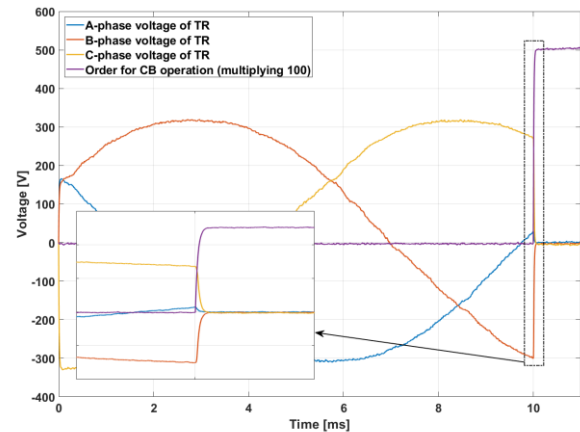
$$\begin{cases} \alpha = 0^\circ : t_o = 16.67 [ms] - t_d \\ \alpha = 90^\circ : t_o = 4.17 [ms] - t_d \end{cases} \quad (9)$$

where t_o is the time for sending the operating signal. t_d is the compensating time delay of the control logic.

The operating delay of each thyristor switch is verified experimentally by applying approximately 30 V from a DC



(a)



(b)

Fig. 7. Test result of operations after compensating time delay for thyristor switches in the laboratory-scale test system: (a) Close; and (b) Open.

power supply and checking the time lag after ordering the thyristor switches to turn on. In Fig. 6, the thyristor switch is considered to be completely open when the voltage across it coincides with the signal for the operating state of the CB at the Vout terminal.

The time lags of approximately 15~20 us are recorded. Therefore, the average value for all closing delays of thyristor switches is set as the compensating time delay of the control logic. After modifying the control logic on to, the operation of the thyristor switch is checked again in the laboratory-scale test system. The thyristor switch operates well when it is commended to be open and closed at the zero point of A-phase voltage as shown in Fig. 7.

B. Residual Flux

Considering the magnetizing characteristic and the structure of the iron core, the residual flux is regulated with a DC power supply. Because the residual flux in the iron core is unknown, it is necessary to make the residual flux identical before every measurement of the inrush current by de-/re-magnetization [17]–[19].

The DC power supply is connected between the A-phase terminal and the neutral terminal at the LV side of the transformer. The transformer is demagnetized first to remove the unknown residual flux in the iron core. The current from the DC power supply is decreased from the initial value step by step as alternating positive and negative values, i.e. +1 A, -1 A, +0.8 A, -0.8 A, . . . , +0.2 A, -0.2 A, +0.05 A, -0.05 A. The magnitude of each DC current is maintained to flow into the transformer for 30 sec.

After eliminating the residual flux by the demagnetization, the DC current should be injected to make the desired residual flux. The hysteresis loop of the electrical steel, 30PH105, for the iron core can determine the residual flux in Fig. 8 [20].

Among the three hysteresis loops presented in Fig. 8, the middle one is chosen to clarify the value of the residual flux though the residual flux can be set arbitrarily. The selected hysteresis loop has 1.5 T as the maximum magnetic flux density and 0.73 T as the residual flux density, respectively.

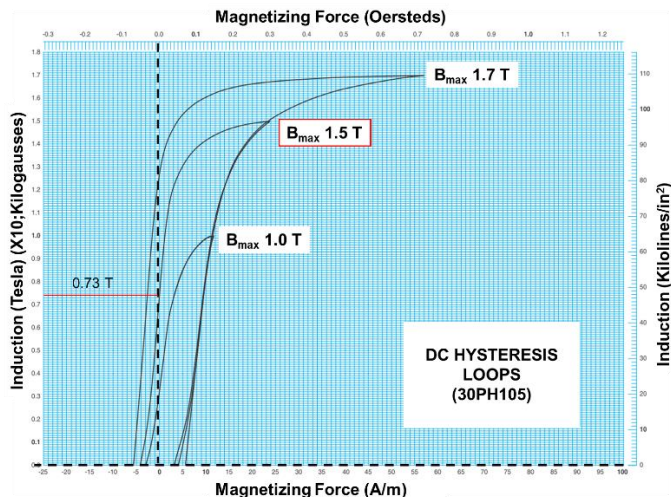


Fig. 8. Hysteresis loops of electrical steel (30PH105).

In other words, if the DC power supply is disconnected after the maximum magnetic flux density, 1.5 T, is achieved by the current, the magnetic flux density varies to its residual flux, 0.73 T, along the hysteresis loop. Moreover, the residual flux density, 0.73 T, is approximately 67 % of the rated magnetic flux density, 1.0907 T in Table II. The ratio, 67 %, is very close to one of the maximum residual flux density, 70 % of the rated magnetic flux density in the worst condition. Therefore, the magnitude of the DC current is calculated in (10) to make the maximum magnetic flux density, 1.5 T, once.

$$I = \frac{S\phi}{N} = \frac{S \cdot B \cdot A}{N} \quad (10)$$

where I is the magnitude of the DC current. S is the reluctance calculated from the structure of the iron core. ϕ is the magnetic flux, and it is equal to the product of the required magnetic flux density, B , and the area of the iron core, A . In this case, B is 1.5 T. N is the number of turns on the side where the DC current is injected. Consequently, the magnitude of the required DC current is determined as approximately 0.94 A by (10).

IV. ANALYSIS OF INRUSH CURRENT

A. Proposed Process and Improved Test System

Before measuring the inrush current repeatedly, the validity of the described ways to control the energizing condition of the transformer is verified. The transformer is energized in the case that the closing instant of the A-phase voltage is 90° , and no residual flux is in the leg of the iron core encircled by the A-phase winding. This energizing condition may make the inrush current of the A-phase minimal. As the measurement results in Fig. 9, the inrush current of the A-phase is almost zero as expected. Therefore, the applied ways are valid in controlling the energizing condition of the transformer.

Finally, the accurate measurement of the inrush current and its comparison with the calculated values from the equations are conducted by following the flow chart shown in Fig. 10. Correspondingly, the initial laboratory-scale test system in

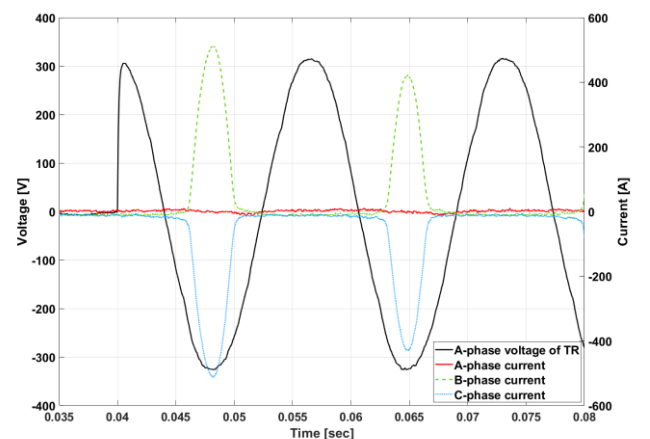


Fig. 9. Measured waveform of A-phase voltage and line currents by controlling the energizing condition (90° for closing instant and demagnetization).

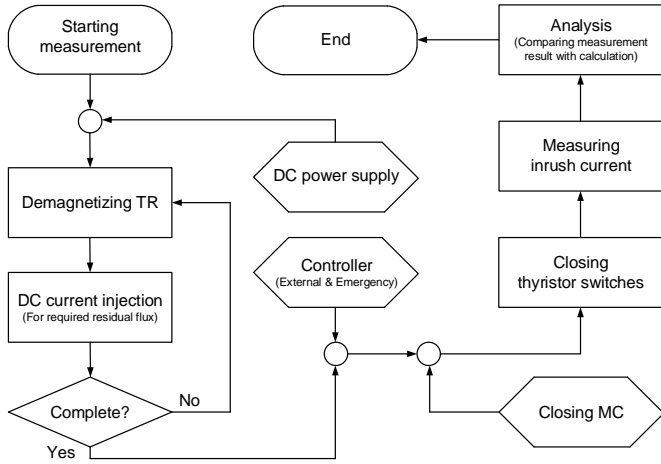


Fig. 10. Flow chart of the proposed process.

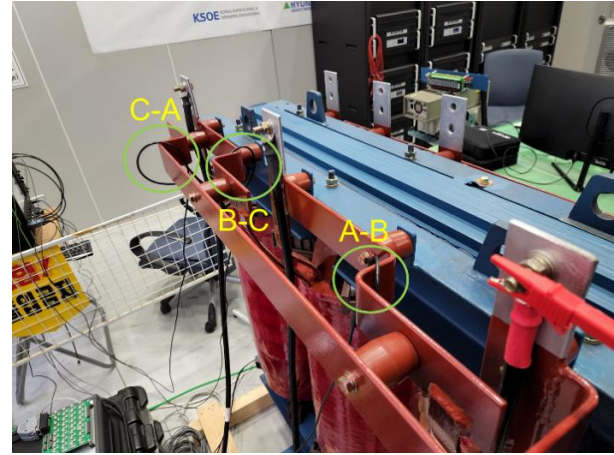


Fig. 13. Installation of CTs to measure phase currents at the delta-connected HV winding.

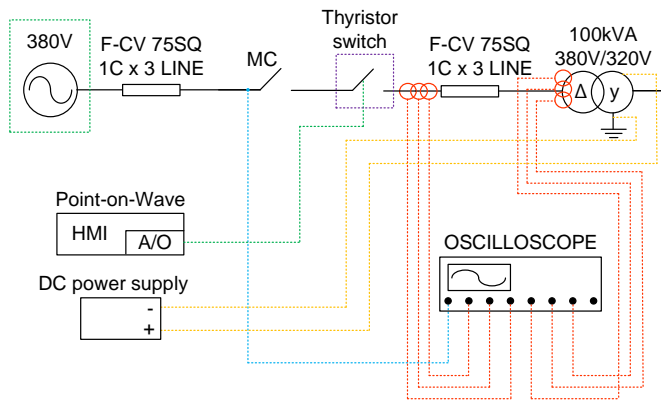


Fig. 11. Configuration of an improved laboratory-scale system.

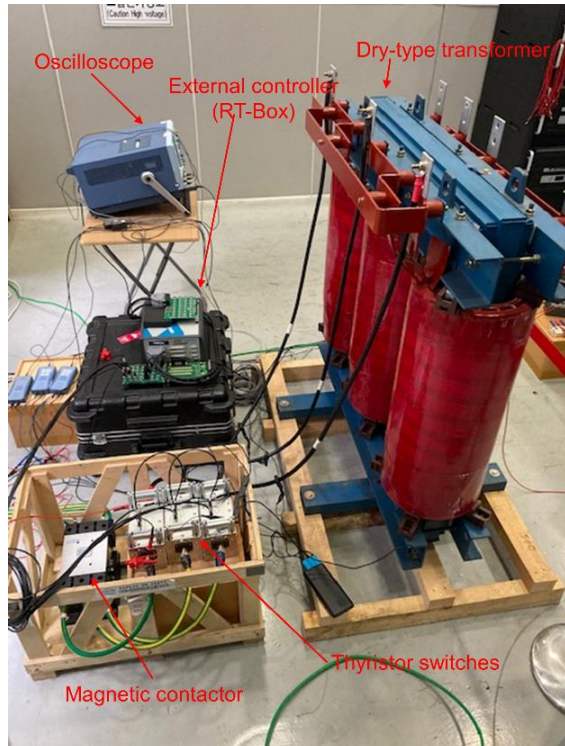


Fig. 12. Organization of the improved laboratory-scale system.

Fig.1 is also improved as Fig. 11 due to the application of the ways to control energizing condition of the transformer. The laboratory-scale test system is organized actually as shown in Fig. 12. The thyristor switches are located between the transformer and the MC. This existing MC is not removed to use it for the galvanic isolation. An 8-channel oscilloscope instead of a 4-channel is also installed in the test system for measuring both line and phase currents simultaneously. The inrush current calculated by (8) is the phase current as the phase voltage is divided by the impedance in these equations. Three current transformers (CTs) record the phase currents at the marked position of the delta-connected HV winding in Fig. 13.

B. Comparison

The inrush current is analyzed by comparing the measurement results with the calculated peak value of the inrush current. The measured inrush currents are approximately ten times of the rated current ($124 \text{ A} = \sqrt{2} \times 88 \text{ A}$ in Table I) by the proposed process in Fig. 10. For all the measurements, the controller is tuned so that the thyristor switch can energize the transformer at 0° for the closing instant of the voltage. After

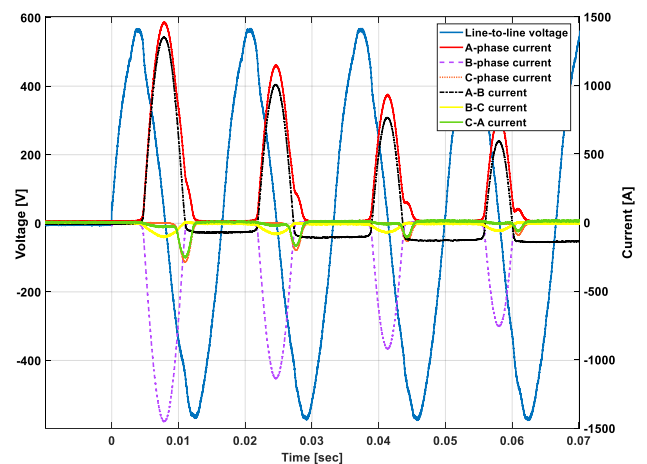


Fig. 14. Measurement of voltage and inrush currents (3 line currents and 3 phase currents) with an oscilloscope.

TABLE III
ANALYSIS OF INRUSH CURRENT

Case No.	Cal. (A)	Meas. (B)	100·B/A
1	1673.74 [A]	1352.23 [A]	80.79 [%]
2		1388.68 [A]	82.97 [%]
3		1401.91 [A]	83.76 [%]
4		1327.36 [A]	79.31 [%]
5		1383.00 [A]	82.63 [%]
6		1335.24 [A]	79.78 [%]
7		1331.41 [A]	79.55 [%]
8		1318.94 [A]	78.80 [%]
9		1291.92 [A]	77.19 [%]
10		1378.68 [A]	82.37 [%]
Mean	1673.74 [A]	1350.94 [A]	80.71 [%]

the demagnetization of the transformer, 0.94 A of the DC current is also injected to make the predetermined residual flux density, 0.73 T, which is approximately 67 % of the rated magnetic flux density. One out of ten measurements is the following waveform for one voltage and six currents (3 line currents and 3 phase currents) in Fig. 14. From those six currents, the maximum phase current is selected for the measurement result in Table III.

Concerning the energizing condition of the equation, the closing instant of the voltage is already 0° in (8) for as mentioned in section II. Therefore, the value of the residual flux density, B_R , have only to be assumed as 67 % of the rated magnetic flux density, B_N , in Table I.

The saturation flux density, B_S , is determined as 2.04 T based on the characteristics of the material. The air-core inductance can be derived from the internal structure of the transformer. Table IV presents the parameters used to calculate the inrush current. According to (8), the maximum inrush current for the transformer in the laboratory-scale test system is 1902.38 A at $t_n = 0$ ms. Additionally, the first peak of the inrush current waveform at $t_n = 8.33$ ms, which represents the first half cycle of the voltage closing at the phase of 0° and the point of maximum magnetic flux, is 1673.74 A as shown in Table III. It is important to note that the system impedance has been disregarded because the main transformer in the laboratory power network has a capacity that is 12.5 times larger than the 100 kVA transformer used for the inrush current tests, assuming a robust network. The implications of this disregard are discussed in the following subsection.

The values of the maximum phase currents and the calculated current are presented in Table III. The inrush current of the transformer is also analyzed to check the difference between the measurement and the calculation. The mean value of the measured inrush currents is 1350.94 A, and its standard deviation is 35.77 A. Consequently, the inrush current measured is approximately 81 % of the peak value calculated.

TABLE IV
PARAMETERS FOR TRANSFORMER INRUSH CURRENT CALCULATION

Parameters	Description	Value
U	RMS voltage [V]	380
R	winding resistance [Ω]	0.0183
L	air-core inductance [mH]	0.5967
B_N	rated magnetic flux density [T]	1.0907
B_R	residual flux density [T]	0.73
B_S	saturation flux density [T]	2.04
t_n	time variable [ms]	8.33

C. Discussion

Significant differences have been observed between the experimentally measured inrush currents and those calculated using (8) due to several factors. One possible reason for these differences is that the calculation of inrush current is based on an ideal condition, as described in (8), which neglects the impedance of the power system and cable. This ideal condition is hard to account for voltage drop and the corresponding decrease in magnetic flux, which are important factors that can affect the magnitude of the inrush current.

Another possible reason for the observed differences is the procedure used to define the parameters in (8), such as the air-core inductance. These formulas are widely used to estimate inrush current, and various parameters can be easily determined based on the transformer's design. However, inaccuracies or imprecision in these parameters can lead to significant differences between predicted and measured inrush currents.

The quality of the experimental setup and the accuracy of the measuring instruments can also contribute to differences between the calculated and measured inrush currents. The experimental setup should be carefully designed and constructed to minimize errors due to stray magnetic fields or other sources of interference. Additionally, the measuring instruments must be accurate and properly calibrated to ensure reliable and repeatable measurements.

V. CONCLUSION

This paper proposes a process to analyze the calculated magnitude of the inrush current by measuring it precisely. To improve the measurement accuracy, both the closing instant of the applied voltage and the residual flux of the iron core are controlled as the proposed process. As a result of verification, the applied ways are obviously effective to measure the inrush current under the required energizing condition.

Finally, the measured peak values of the inrush current are approximately 81 % compared to the calculated value. In summary, significant differences between the calculated and measured inrush currents in transformers can be attributed to a variety of factors, including the ideal conditions assumed in the calculation, inaccuracies in the parameters used, and errors

in the experimental setup or measuring instruments. These factors should be carefully considered when interpreting inrush current measurements and designing transformer. Nevertheless, it can be concluded that the widely used equation is quite inaccurate to calculate the magnitude of the inrush current.

[20] POSCO, *ELECTRICAL STEEL*, 6261, Donghaean-ro, Nam-gu, Pohang-si, Gyeongsangbuk-do, Republic of Korea.

VI. REFERENCES

- [1] N. Chiesa and H. K. Høidalen, "Systematic switching study of transformer inrush current: simulations and measurements," in *International Conf. on Power Systems Transients 2009 - IPST 2009*, June 2009.
- [2] N. Chiesa, B. A. Mork, and H. K. Høidalen, "Transformer model for inrush current calculations: Simulations, measurements and sensitivity analysis," *IEEE Transactions on Power Delivery*, vol. 25, no. 4, pp. 2599–2608, 2010.
- [3] Cigre and W. G. C4.307, "Cigre technical brochure 568 transformer energization in power systems: A study guide," *Cigre*, 2014.
- [4] J. E. Holcomb, "Distribution Transformer Magnetizing Inrush Current," in *Transactions of the American Institute of Electrical Engineers. Part III: Power Apparatus and Systems*, vol. 80, no. 3, pp. 697-702, 1961.
- [5] T. R. Specht, "Transformer Inrush and Rectifier Transient Currents," in *IEEE Transactions on Power Apparatus and Systems*, vol. PAS-88, no. 4, pp. 269-276, 1969.
- [6] Cigre and W. G. B2.36, "Cigre technical brochure 569 resonance and ferroresonance in power networks," *Cigre*, 2014.
- [7] S. I. Kim, B. C. Sung, S. N. Kim, Y. C. Choi, and H. J. Kim, "A study on ferroresonance mitigation techniques for power transformer," in *International Conf. on Power Systems Transients 2015 - IPST 2015*, June 2015.
- [8] M. Bonislawski, M. Hołub, P. Waszczuk, and W. Lewanski, "Automated test stand for transformer inrush current measurement," in *2018 14th Selected Issues of Electrical Engineering and Electronics (WZEE)*, 2018, pp. 1–4.
- [9] N. Chiesa and H. K. Høidalen, "Novel approach for reducing transformer inrush currents: Laboratory measurements, analytical interpretation and simulation studies," *IEEE Transactions on Power Delivery*, vol. 25, no. 4, pp. 2609–2616, 2010.
- [10] W. Chandrasena, D. Jacobson, and P. Wang, "Controlled switching of a 1200 mva transformer in manitoba," *IEEE Transactions on Power Delivery*, vol. 31, no. 5, pp. 2390–2400, 2016.
- [11] J. Mitra, X. Xu, and M. Benidris, "Reduction of three-phase transformer inrush currents using controlled switching," *IEEE Transactions on Industry Applications*, vol. 56, no. 1, pp. 890–897, 2020.
- [12] S. Fang, H. Ni, H. Lin, and S. L. Ho, "A novel strategy for reducing inrush current of three-phase transformer considering residual flux," *IEEE Transactions on Industrial Electronics*, vol. 63, no. 7, pp. 4442–4451, 2016.
- [13] Y. Pan, X. Yin, Z. Zhang, B. Liu, M. Wang, and X. Yin, "Three-phase transformer inrush current reduction strategy based on prefluxing and controlled switching," *IEEE Access*, vol. 9, pp. 38 961–38 978, 2021.
- [14] S.-D. Chen, R.-L. Lin, and C.-K. Cheng, "Magnetizing inrush model of transformers based on structure parameters," *IEEE Transactions on Power Delivery*, vol. 20, no. 3, pp. 1947–1954, 2005.
- [15] S. V. Kulkarni and S. A. Khaparde, *Transformer engineering: design and practice*, 1st ed. 270 Madison Avenue, New York, NY 10016, USA: Marcel Dekker, 2004.
- [16] S. V. Kulkarni and S. A. Khaparde, *Transformer engineering: design, Technology, and Diagnostics*, 2nd ed. 6000 Broken Sound Parkway Northwest, Suite 300 Boca Raton, Florida, FL 33487, USA: CRC Press, 2013.
- [17] B. Kovan, F. de Leon, D. Czarkowski, Z. Zabar, and L. Birenbaum, "Mitigation of inrush currents in network transformers by reducing the residual flux with an ultra-low-frequency power source," *IEEE Transactions on Power Delivery*, vol. 26, no. 3, pp. 1563–1570, 2011.
- [18] D. M. Robalino, "Power transformer demagnetization," in *2016 IEEE 36th Central American and Panama Convention (CONCAPAN XXXVI)*, 2016, pp. 1–5.
- [19] A. Ahföck and A. Hewitt, "DC magnetisation of transformers," *Electric Power Applications, IEE Proceedings -*, vol. 153, pp. 601 – 607, 08 2006.